

# We are IntechOpen, the world's leading publisher of Open Access books Built by scientists, for scientists

7,000

Open access books available

186,000

International authors and editors

200M

Downloads

Our authors are among the

154

Countries delivered to

TOP 1%

most cited scientists

12.2%

Contributors from top 500 universities



WEB OF SCIENCE™

Selection of our books indexed in the Book Citation Index  
in Web of Science™ Core Collection (BKCI)

Interested in publishing with us?  
Contact [book.department@intechopen.com](mailto:book.department@intechopen.com)

Numbers displayed above are based on latest data collected.  
For more information visit [www.intechopen.com](http://www.intechopen.com)



---

# Analytical and Mathematical Analysis of the Vibration of Structural Systems Considering Geometric Stiffness and Viscoelasticity

---

Alexandre de M. Wahrhaftig,  
Reyolando M. L. R. F. Brasil and  
Lázaro S. M. S. C. Nascimento

Additional information is available at the end of the chapter

<http://dx.doi.org/10.5772/intechopen.75615>

---

## Abstract

For a complete analysis of vibration, the stiffness of a structure must have two characteristics: one corresponding to conventional stiffness and the other to the geometric stiffness. Thus, the total stiffness takes form where the model to be used to represent any behavior of the material is introduced to the first part via the modulus of elasticity. The second is the geometric stiffness, through which it is possible to linearize a geometric nonlinear problem. To consider both aspects, a mathematical model based on the Rayleigh method has been elaborated. Two systems were numerically studied. First, the occurrence of resonance in the vibration of a prestressed reinforced concrete beam has been investigated. The results indicated resonant and non-resonant schemes between the natural frequency of the beam and the frequency of the engine. To the second system, the first natural frequency of a slender, 40-m-high concrete mobile phone mast, was calculated, and an evaluation of the structural collapse was performed. To the both systems, the cross section of reinforced concrete was treated by the theory for the homogenized section in order to consider the presence of the steel, and the viscoelasticity of the concrete was taken into account through a three-parameter rheological model.

**Keywords:** analytical mathematical analysis, numerical simulation, viscoelasticity, vibration, rheology, Rayleigh method, geometric stiffness, buckling load

---

## 1. Introduction

The dynamic characteristics of a structure depend, basically, on its stiffness and mass. With these two elements, the natural frequencies and modes of vibration of the system are determined. However, the initial stiffness of a structure can be affected by the so-called geometric stiffness, a function of the acting normal force. In the case of compression force, the stiffness of the structure decreases, also reducing the natural frequencies of vibration. A class of structures of socio-economic-strategic importance for the national industry are machine bases, which are subject to vibrations induced by the supported equipment. These vibrations can affect the safety of the structure itself and generate detrimental effects on the equipment and the quality of the manufactured product. They can also make the working ambience unsuitable for operators. All industrial sectors are subject to these problems, including oil exploration, production, and refining, mining, wind energy, atomic energy, as well as bridges and viaducts for road and rail use.

Although equipment support structures are, as a general rule, over-dimensioned, and therefore not subject to the effects of geometric stiffness, the tendency of modern structural engineering is towards increasingly slender elements, made possible by materials that are more efficient and lightweight, and having more and more powerful structural analysis capabilities. One of these features is prestressed concrete, represented by the presence of a steel bar or cable inside the structure that compresses it, the purpose of which is to reduce the effects of tension on flexion. In the case of beams subjected to periodic excitation, it is assumed that the original design has taken care to distance the natural frequencies of the system from those of the excitation, considering that, by hypothesis, the prestressing force decreases the stiffness of the element and, consequently, its natural frequencies, which may lead to unexpected, potentially dangerous resonance regimes. In the opposite direction, the presence of the prestressing can provide a form of control of this same vibration, where a resource is available to remove the structure of the resonant regime, if perceived in the preliminary stages of design. In one way or another, a satisfactory analysis solution to most engineering problems comes from a consideration that is easily implemented in analytical and numerical-computational formulations: the geometric stiffness. The influence of geometric stiffness has been studied in several contexts, both in laboratory tests and in comparison with the finite element method (FEM) [1–4].

The problem is aggravated when the material itself changes its elastic properties, such as in the case of viscoelasticity, which represents the gradual increase of deformation with time. This is a typical phenomenon of concrete structures because it is a viscoelastic material. It must be considered when verifying the stability of slender pieces compressed under the ultimate limit state (ULS), since these have their stiffness modified in function of the rheology of the material itself. It is important to consider the viscoelastic behavior of concrete structures relative to the characteristics of the structural element under study; this is necessary when verifying the stability of compressed slender pieces, since their stiffness is modified according to the rheology of the material. For this reason, in the specific case of columns in that loading condition, a premature analysis can produce undesired consequences, and the system may even collapse.

Typically, viscoelasticity representation is based on rheological models that are associated with deformations that are deferred over time. These models can be included in a static or dynamic analysis of the structures by relating them to the modulus of elasticity of the material. In the case of dynamic analysis, the stiffness of the structure must be composed of two terms, one of which corresponds to the portion of conventional stiffness and the other to the geometric stiffness parcel [5]. Thus, it is possible to introduce into the first one a modulus of elasticity that is variable over time, according to the rheological model adopted, keeping the stress level constant, and, in the second, to consider the normal stress acting on the system, which includes the self-weight of the structural element. An approximate and satisfactory solution can be found by considering viscoelasticity through flexural bending over time.

To evaluate these aspects, a numerical simulation has been performed, assuming an idealized section of a beam as an engine base. A rheological model of the three parameters has been used to obtain the variable modulus of elasticity. A model, including geometric stiffness, distributed, and concentrated masses, is derived based on the Rayleigh method and solved for a range of axial compression load values. The results made it allowed us to verify the resonant and non-resonant response of the system. A second analysis has been performed to simulate numerically the variation of the first natural frequency of vibration of an actual structure of reinforced concrete, axially loaded, and considering also the viscoelasticity by means of the same rheological model. The loss of stability of the system has been then evaluated.

## 2. Mathematical solution for representing the viscoelasticity

An increase in strain over time under constant stress is a viscoelastic phenomenon. Mathematically, viscoelasticity can be represented by a time-dependent function associated with rheological models capable of describing the phenomenon [6]. The slow deformation for concrete parts is a phenomenon that is related to loads and deformations but is partially reversible [7]. It is a phenomenon that is directly related to the movement of moisture inside concrete. When a sample of concrete is loaded for 90 days and then unloaded, the immediate or elastic recovery is approximately the same magnitude as the elastic deformation when the first load is applied [8].

It is conceptually convenient to consider classic viscoelastic models in which only two types of parameters, relating to elasticity and viscosity, appear [9]. Classic viscoelastic models are obtained by arranging springs and dampers, or dashpots, in different configurations. Springs are characterized by elastic moduli and dashpots by viscosity coefficients. The best known of these mechanical models are the Maxwell model, containing a spring in series with a dashpot, and the Kelvin-Voigt model, containing a spring and dashpot in parallel. One model used to represent the viscoelasticity of solids is the three-parameter model, in which the elastic parameter  $E_0$  is connected to the viscoelastic Kelvin-Voigt model with parameters  $E_1$  and  $\eta_1$ , which is a simplification of the Group I Burgers model, as shown in **Figure 1**.

The three-parameter model sufficiently describes the viscoelastic nature of many solids and is often used to study the phenomenon in various scientific fields. The total deformations of the

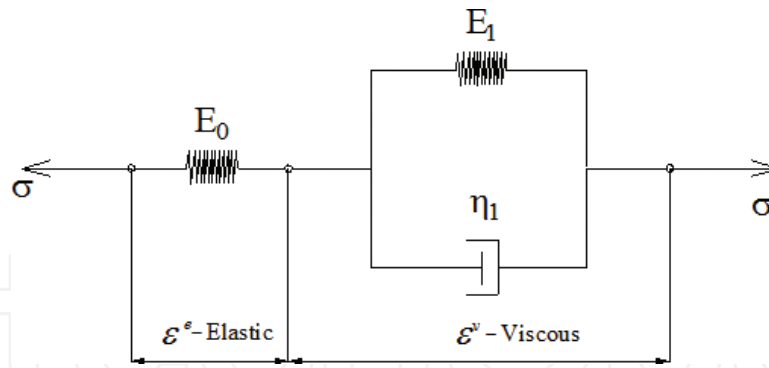


Figure 1. Viscoelastic model of three parameters.

Kelvin-Voigt model are given by  $\varepsilon = \varepsilon^e + \varepsilon^v$ , where  $\varepsilon^e$  is the deformation of the elastic model, and  $\varepsilon^v$  is the deformation of the Kelvin-Voigt model. When differentiated with respect to time, the total deformation is obtained as

$$\dot{\varepsilon} = \dot{\varepsilon}^e + \dot{\varepsilon}^v \quad (1)$$

which is the constitutive equation of the elastic and Kelvin-Voigt models, respectively. Considering  $E_1 = E_0$  as the modulus of elasticity for both parts of the rheological model,

$$\sigma = E_0 \varepsilon^e \text{ and } \dot{\sigma} + \frac{E_0 + E_0}{\eta_1} \sigma = E_0 \dot{\varepsilon} + \frac{E_0 E_0}{\eta_1} \varepsilon \quad (2)$$

are found. From the previous equations, one derives the following differential equation:

$$\sigma = E_0 \varepsilon^v + \eta_1 \dot{\varepsilon}^v \quad (3)$$

where  $\sigma = 0$  for  $t < 0$  and  $\sigma = \sigma_0$  for  $t > 0$ , with  $t$  representing the time and  $t = 0$  the instant of loading application. As the stress remains constant, the stress derivate with respect to time is zero. Applying the previous stress condition, the following ordinary differential equation is found:

$$E_0 \dot{\varepsilon} + \frac{E_0 E_0}{\eta_1} \varepsilon = \sigma_0 \quad (4)$$

for which the general solution for  $t > 0$ , taking the initial condition  $\varepsilon(0) = \sigma_0/E_0$ , is

$$\varepsilon(t) = \sigma_0 \left[ \frac{1}{E_0} + \frac{1}{E_0} \left( 1 - e^{-\frac{E_0}{\eta_1} t} \right) \right] \quad (5)$$

Obviously, if the stress level remains constant, the modulus of elasticity should decrease concurrently with increasing strain:

$$E(t) = \frac{1}{\frac{1}{E_0} + \frac{1}{E_0} \left( 1 - e^{-\frac{E_0}{\eta_1} t} \right)} \quad (6)$$

The previous solution for consideration of the viscoelastic behavior of materials was used by [10] to evaluate the stability of a slender wooden column, for example. However, it is of interest, at this moment, to make clear that the present work is a numerical approximation, which takes into account the viscoelastic behavior of the concrete by assuming a viscoelastic rheological model of three parameters or as also is known of the solid standard.

It is important to note that the viscoelastic behavior of the considered material is completely represented by the temporal modulus of elasticity. Therefore, the solid such behavior is wished to study should be according that adopted model. Any material can be represented by it, being, however, its usage conditioned by performing of experimental studies in order to confirm if it is correct or not. Keeping this in mind, the concrete viscoelastic behavior is assumed to be represented by the solid standard model, as an approximation of the reality. However, criteria from regulatory codes can be used in substituting of that model or even any other rheological models can be adopted.

### 3. Beam as a basis of supporting

#### 3.1. Basic considerations prestressing in reinforced concrete

A piece can be considered as prestressed reinforced concrete when it is subjected to the action of the so-called prestressing forces and of permanent and variable loads, so that the concrete is not subjected to tension or it occurs below the limit of its resistance. As an example, take the normal stresses beam diagrams of the prestressed beam of **Figure 2**, where  $P$  is the prestressing force,  $M_P$  the bending moment due to eccentricity of the load  $P$ ,  $M_p$  is the bending moment due to uniformly distributed load  $p$  and  $R$  is the resultant, each one of these with their corresponding normal stresses. Under the conditions presented, the lower fibers of the beam, under positive bending moment, will have the tension stresses overturned by the superposition of those produced by the normal stress of the applied stress eccentrically.

Prestressed concrete was developed scientifically from the beginning of the last century. Prestressing can be defined as the artifice of introducing, in a structure or a part, a previous state of stresses, in order to improve its resistance or its behavior in service, under the action of

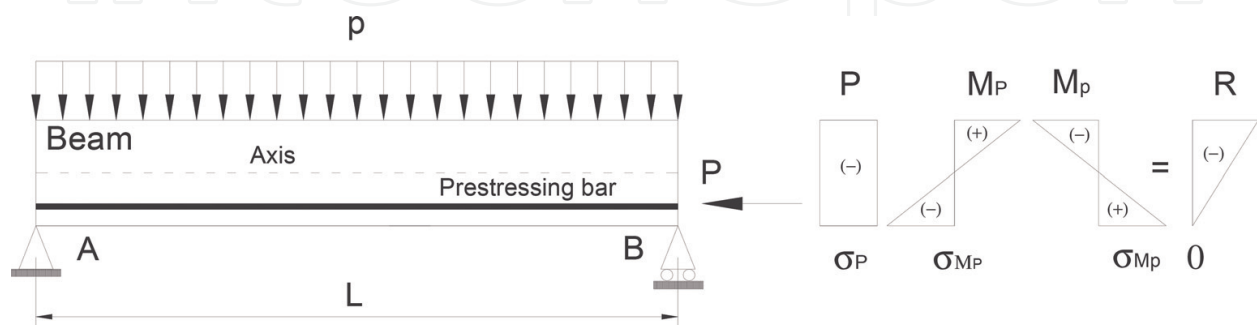


**Figure 2.** Normal stresses in a prestressed beam.



several effects. Due to the characteristics of the concrete as a structural material, the use of prestressing can bring a great advantage from the economic point of view. When comparing the cost of a prestressed structure with a similar one of conventional reinforced concrete, there is a reduction in the final cost of the structure due to the reduction of steel reinforcement [11]. In addition, the prestressing allows the part to overcome large spans, improves the control and reduction of deformations and fissures. It can also be used for structural recovery and reinforcement, as well as for slender systems and prefabricated or precast parts. There are three types of prestressing systems: (1) prestressing with initial adherence, (2) prestressing with posterior adherence, and (3) prestressing without adherence. The latter type is composed of a post-tensioning system characterized by the slipping freedom of the steel reinforcement in relation to the concrete, along the whole extension of the cable, except for the anchorages.

In a non-adherent prestressing, the cables or chutes are wrapped in two or three layers of resistant paper. The wires and paper are painted with bituminous paint in order to tension them after the concrete has hardened. The bitumen avoids the penetration of the cement cream inside the cable and, in this way, it eliminates adhesion between the concrete and the reinforcement [12]. The prestressed concrete is a composite material of the aggregate mixture and a cement paste associated with prestressing cables and/or passive reinforcing bars. Because of the combination of several materials, these structures develop a highly complex behavior, presenting a non-linear response, which is due, among other factors, to time-dependent effects, such as the creep of the concrete [13].

### 3.2. Mathematical model for the nonlinear vibration problem

Consider a rotary machine mounted on a beam subjected to a pre-tensioning force, without adhesion. It is known that such forces affect the geometric stiffness and, consequently, the values of the undamped free-vibration frequencies. If the structure is designed, as is usually the case, to have frequencies farther from the machine's service speed rotation, the changes in the frequency due to geometric stiffness may lead to the appearance of potentially dangerous resonance conditions.

Take a beam model of Bernoulli-Euler applied to a simply supported beam  $AB$  of length  $L$  and inertia  $I$ , intended to function as the base of an engine  $E_g$ , composed of viscoelastic material, represented by the temporal modulus of elasticity  $E(t)$  as shown in **Figure 3**. A normal force of compression  $P$  reproduces the post-tensioning force, which changes the stiffness, and consequently, the natural frequency of vibration of the structure with time. The eccentricity between

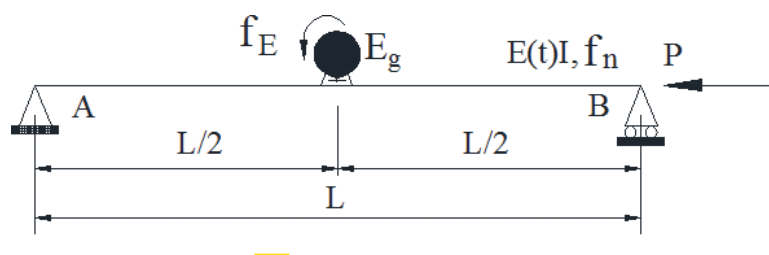


Figure 3. Beam model.

the engine axis and the part is initially ignored. The vertical displacement of the central joint is the generalized coordinate of the system.

By using the Rayleigh method [14], the undamped vibration frequency in its first mode considering viscoelasticity is obtained. It is worth mentioning that Rayleigh assumed that a system containing infinite degrees of freedom could be associated with another with a single degree of freedom (SDOF) to approximate its frequency. It is important to note that the technique developed by Rayleigh aimed at calculating the fundamental vibration frequency of elastic systems, as its precision is dependent on the function chosen to represent this mode of vibration.

The basic concept of the method is the principle of energy conservation, and can, therefore, be applied to linear and nonlinear structures. [15] applies the Rayleigh technique to determine the fundamental period of vibration to verify the stability of mechanical systems. The process is described in relation to the principle of virtual works and as the appropriate choice of the generalized coordinate describing the first mode of vibration. At the end of the process, the generalized properties of the system are obtained as stiffness and mass, necessary for the calculation of the frequency.

Consider that the vertical displacement of a generic section of the beam in **Figure 4** is given by:

$$v(x, t) = \phi(x) q(t), \quad (7)$$

in which  $\phi(x)$  is a shape function that attempts to define the boundary conditions in the supports and value 1 in the central section of the beam, whose displacement with time is  $q(t)$ . In this case, one adopts the shape function  $\phi(x) = \sin(\pi x/L)$ , which is the exact solution of the problem without the  $P$  load. A prime mark will denote a derivative of the function in relation to  $x$  (Lagrange's notation).

Applying the Rayleigh method, one has the conventional bending stiffness,  $K_0$ , as a function of the material behavior and the geometry of the cross, which is equivalent to:

$$K_0(t) = \int_0^L E(t) I (\phi'')^2 dx = \frac{\pi^4 E(t) I}{2L^3} \quad (8)$$

where  $E(t)I$  is the known flexural bending with viscoelasticity, represented by multiplication of the temporal material modulus of elasticity with the inertia of the section in relation to the considered movement, the vertical vibration mode (1st mode). In turn, the geometric stiffness,  $K_G$ , as a function of the normal force of compression (or even tension), is equivalent to:

$$K_G = P \int_0^L (\phi')^2 dx = \frac{P\pi^2}{2L} \quad (9)$$

The total generalized mass of the system is found by calculating  $M = M_C + M_V$  where  $M_C$  is the concentrated mass at the middle span and  $M_V$  is the mass coming from the beam self-weight given by:



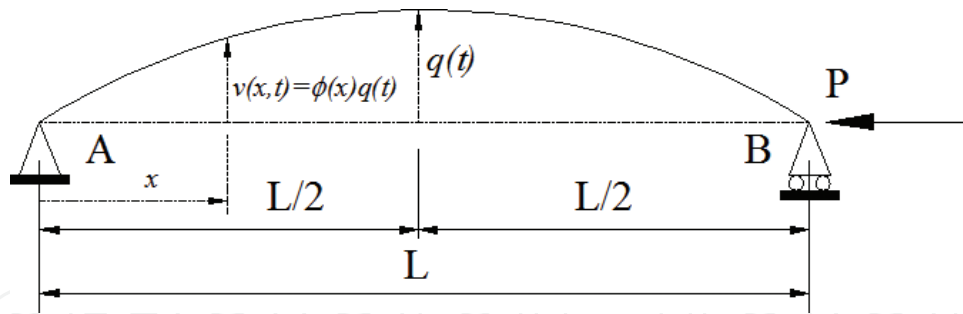


Figure 4. Rayleigh method.

$$M_v = \int_0^L m_V \phi(x)^2 dx = \frac{m_V L}{2} \quad (10)$$

in which  $m_V$  represents the total mass per length unit. Finally, the frequency of undamped free vibration (in rad/s) is found by way of Eq. (11):

$$\omega(t) = \sqrt{\frac{K(t)}{M}} \quad (11)$$

Considering the total beam stiffness as  $K(t) = K_0(t) - K_G$ , the free undamped frequency of vibration of the 1st mode is found, in Hertz, admitting the compressive force as positive, by:

$$f(t) = \frac{\omega(t)}{2\pi} = \frac{1}{2} \left[ \frac{\pi^2 E(t) I - P L^2}{L^3 (L m_V + 2 M c)} \right]^{\frac{1}{2}} \quad (12)$$

For a better understanding of the Rayleigh method and the importance of the geometric stiffness to the structural analysis, the work [16, 17] should be consulted.

### 3.3 Numerical simulation 1

The beam gross cross section was estimated with a passive reinforcement arrangement capable of resisting the predicted load in the simulation, being treated by the homogenized section method, with geometry as indicated in **Figure 5**. The modulus of elasticity of the concrete was calculated according to NBR 6118/2014 [18] recommendations, following Eq. (13), for a concrete characteristic compressive strength,  $f_{ck}$ , equal to 30 MPa.

$$E_0 = \alpha_i \cdot 5600 \sqrt{f_{ck}} = 26838.405 \text{ MPa};$$

$$\alpha_i = 0.8 + 0.2 \cdot \frac{f_{ck}}{80 \text{ MPa}} = 0.875 \quad (13)$$

The reinforced concrete specific weight  $\gamma_c$  was obtained for a material density  $\rho$  of 2500 kg/m<sup>3</sup> and a gravitational acceleration  $g$  of 9.8061 m/s<sup>2</sup>, therefore  $\gamma_c = 24.52$  kN/m<sup>3</sup>.

Section data:

- External height:  $H = 16 \text{ cm}$
- Internal height:  $h = H - 2 \cdot t = 6 \text{ cm}$
- Wall thickness:  $t = 5 \text{ cm}$
- Concrete cover:  $c' = 25 \text{ mm}$
- Reference beam span:  $L = 3 \text{ m}$
- Reinforced bar diameters:  $d_b = 8 \text{ mm}$
- Number of reinforcement bars:  $nb = 4$
- Total inertia:  $I = \frac{H^4 - h^4}{12} = 5353 \text{ cm}^4$
- Gross-sectional area:  $A = H^2 - h^2 = 220 \text{ cm}^2$

The concrete section was homogenized by the transformation of the steel bars of the reinforcement, which led to a homogenization factor of 1.061 to be considered in the material and geometric properties of the beam section. The homogenizing technic is presented in Section 4.2. For the simulation, all the elements that constitute physical parts to be added to the system, such as the bar used in prestressing systems and an electric induction motor that represents periodic excitation, were considered as lumped or distributed masses.

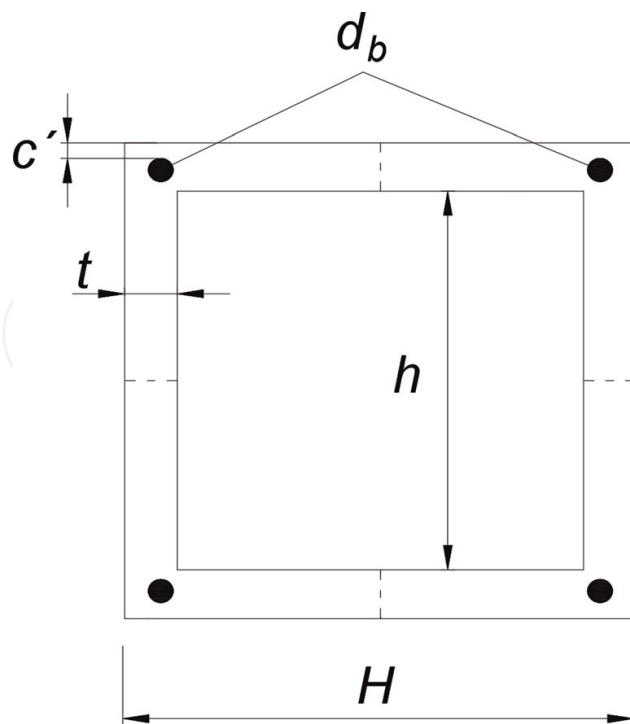


**Figure 5.** Beam section characteristics.

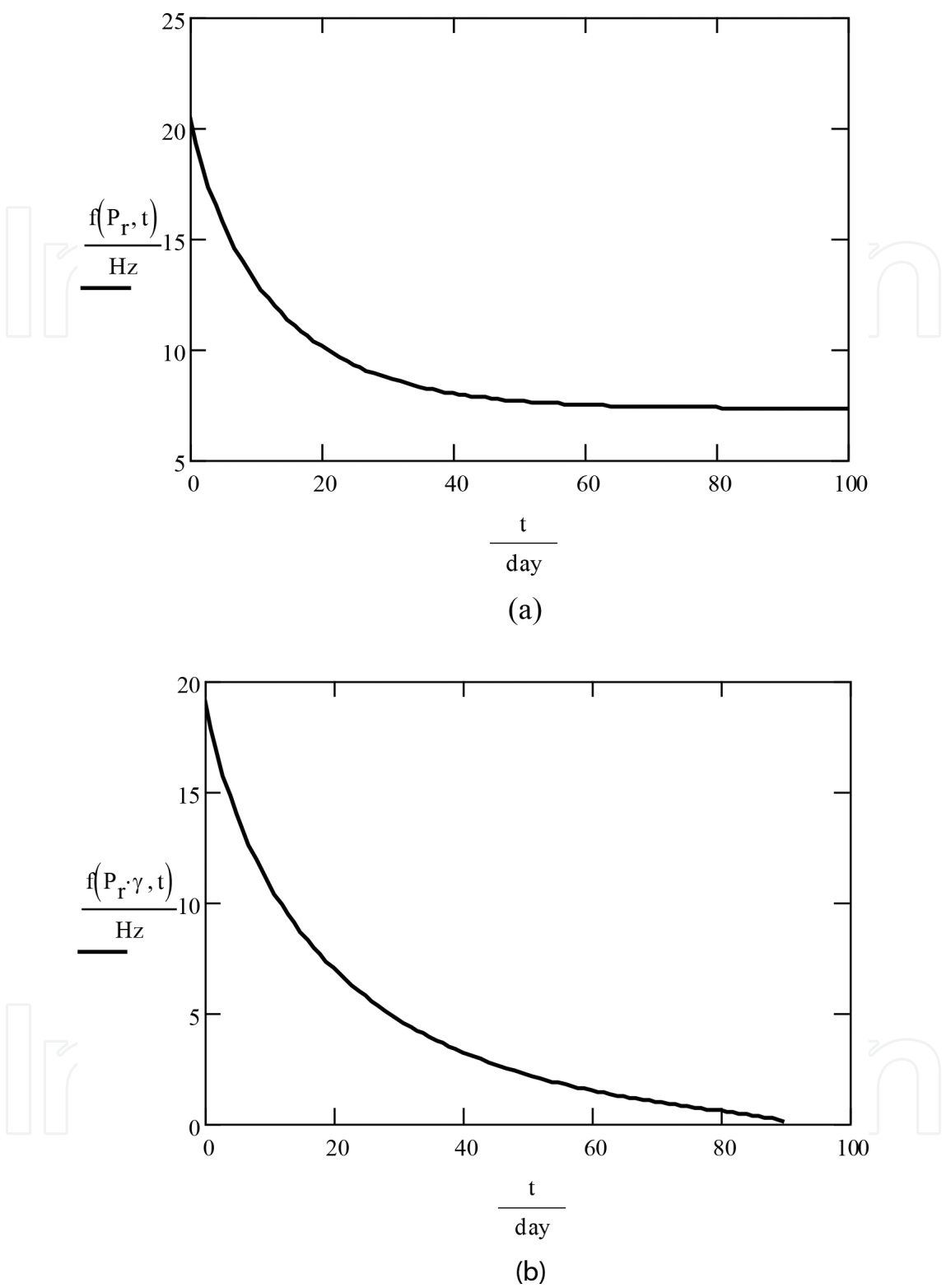


**Figure 6.** Frequency of the beam with time with viscoelasticity. (a) Frequency with time for capacity of the section, (b) Safety factor  $\gamma$ —Collapse at 90th day.

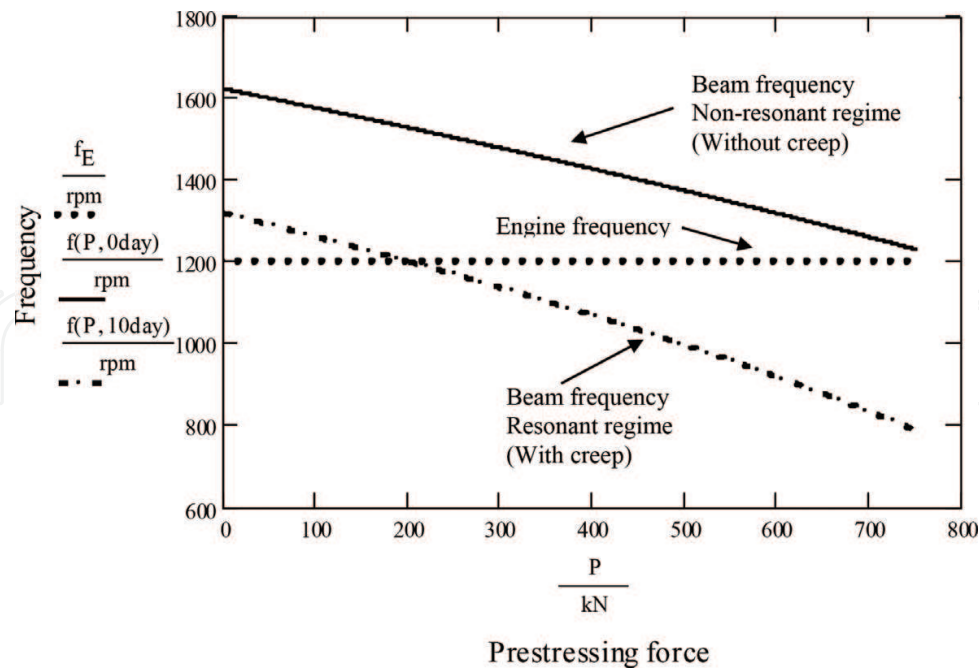


**Figure 7.** Resonant and non-resonant frequencies as a function of axial compression force  $P$ .

By fixing the force on the section-resistant capacity, one can observe the variation of the natural frequency of the beam with time when considering viscoelasticity, as shown in **Figure 6(a)**. A safety factor of 1.170426 to be applied to the loading can be found, which defines the beam collapse at the 90th day, as can be seen in **Figure 6(b)**. By varying force  $P$ , which represents a non-adherent post-tension force, from zero to the resistant capacity of the section, the variation of the natural frequency of the beam is obtained, given in the graph in **Figure 7**. There, it is possible to see that, with the increase of the axial compression force, the beam frequency decreases, since the geometric portion ( $K_G$ ) stiffness is changed, consequently decreasing the total stiffness ( $K$ ) of the beam.

Since the motor rotation is set at 1200 rpm (20 Hz), represented by the dotted horizontal line, there is no resonance without consideration of viscoelasticity, but the resonance appears when the natural frequency of the beam is calculated with the introduction of the viscoelastic behavior of the material. For 10 days after application of load, for example, the resonant regime can be observed by the intersection of two curves, dotted (horizontal) and dashed (sloped), defining exactly for which prestressing force the phenomenon occurs at that instant (210 kN).

## 4. Column as a structure for transmitting system

### 4.1. Formulation of the undamped vibration problem

Assuming the well-known trigonometric function

$$\phi(x) = 1 - \cos\left(\frac{\pi x}{2L}\right), \quad (14)$$

where  $x$  is an independent variable of the problem originating in the base, in the cantilever position, and  $L$  is length of the column,  $q(t)$  is the generalized coordinate, and  $e(t)$  is the vertical displacement of the top due the vibratory movement, as shown in **Figure 8**. By using the Rayleigh method, in a similar way as described in the previous Section 3.2, the conventional stiffness is found by

$$k_{0s}(t) = \int_{L_{s-1}}^{L_s} E(t)I_s F_s (\phi'')^2 dx, \text{ with } K_0(t) = \sum_{s=1}^n k_{0s}(t), \quad (15)$$

where  $k_{0s}(t)$  and  $F_s$  are the parcel of the stiffness and the homogenizing factor of the concrete cross section due to the reinforcement steel at the segment  $s$ .  $K_0$  is the final conventional stiffness, where  $n$  is the total number of intervals given by the structural geometry.  $E(t)$  represents the variable modulus of elasticity on time, according Eq. (6), and  $I_s$  is the moment of inertia of each section.

The geometric stiffness is obtained by the following equation:

$$k_{gs} = \int_{L_{s-1}}^{L_s} N(x) (\phi'')^2 dx, \text{ with } K_g = \sum_{s=1}^n k_{gs}, \quad (16)$$

where  $k_{gs}$  is the geometric stiffness at the interval  $s$ ;  $K_g$  is the total geometric stiffness of the structure, with  $n$  as defined before;  $N(x)$  is a normal effort function at the respective interval,

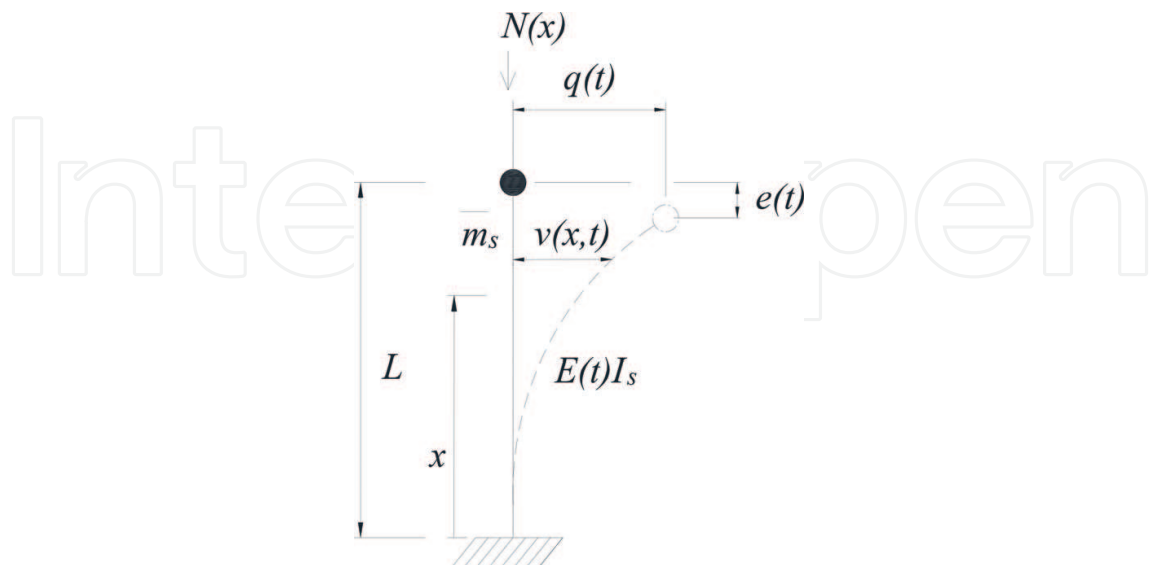


**Figure 8.** Mathematical model of vibration of a column.

which includes the self-weight of the column on considered part, and the lumped forces from upper segments, or better

$$N(x) = \{m_0 + \bar{m}_s[(L_s - L_{s-1}) - x]\}g, \quad (17)$$

with  $m_0$ ,  $\bar{m}_s$  are defined below, and  $g$  is the acceleration of gravity. The generalized mass is then given by  $M = m_0 + m$ , where  $m_0$  is the lumped mass on the top and  $m$  is the generalized mass found with

$$m_s = \int_{L_{s-1}}^{L_s} \bar{m}_s (\phi(x))^2 dx, \text{ with } \bar{m}_s = A_s \rho \text{ and } m = \sum_{s=1}^n m_s, \quad (18)$$

where  $\bar{m}_s$  is the mass to each segment  $s$ , found by multiplying the cross-sectional area  $A_s$  to the density  $\rho$  of the material at the respective intervals, that is,  $\bar{m}_s$ , mass per unit length, and  $m$ , generalized mass of the system due the density of the material, with  $n$  as defined previously. The first natural frequency of the structure is calculated:

$$\omega(t) = \sqrt{\frac{K(t)}{M}} (rd/s) \cdot f(t) = \frac{\omega(t)}{2\pi} (\text{Hertz}), \quad (19)$$

taking into consideration that, for a compressive force being positive, the temporal stiffness is:

$$K(t) = K_0(t) - K_g. \quad (20)$$

It is important to mention that Eq. (14) has been evaluated by [19] as a valid shape for the first mode of vibration with geometric nonlinear characteristics, applied for actual structures, even those with variable geometry, being a function valid throughout the entire domain of the structure.

## 4.2. Numerical simulation 2

A 40-m-high reinforced concrete pole structure with an external 60-cm hollow circular cross-sectional diameter, with variable thickness (**Figure 9**) and a slenderness ratio of 472 was used for analysis. The properties of the sections change along the length due to the changes in thickness and variation of the steel area.

The concrete used in the manufacture of the structure had the compression characteristic strength  $f_{ck}$  of 45 MPa, viscosity  $\eta_1$  of 51089681149.92 MPa·s, and a density  $\rho$  of 2600 kg/m<sup>3</sup>. The concrete cover  $c'$  specified for the reinforcing steel was 25 mm and the steel used in the construction of the pole was CA-50, with yield strength of 500 MPa and modulus of elasticity  $E_s$  of 205 GPa. The secant modulus of elasticity of the concrete  $E_c$  is 31931.05 MPa. The numerical simulation was performed considering that all elastic parameters in Eq. (6) are equal to the modulus of elasticity of the concrete,  $E_0 = E_1 = E_c$ .



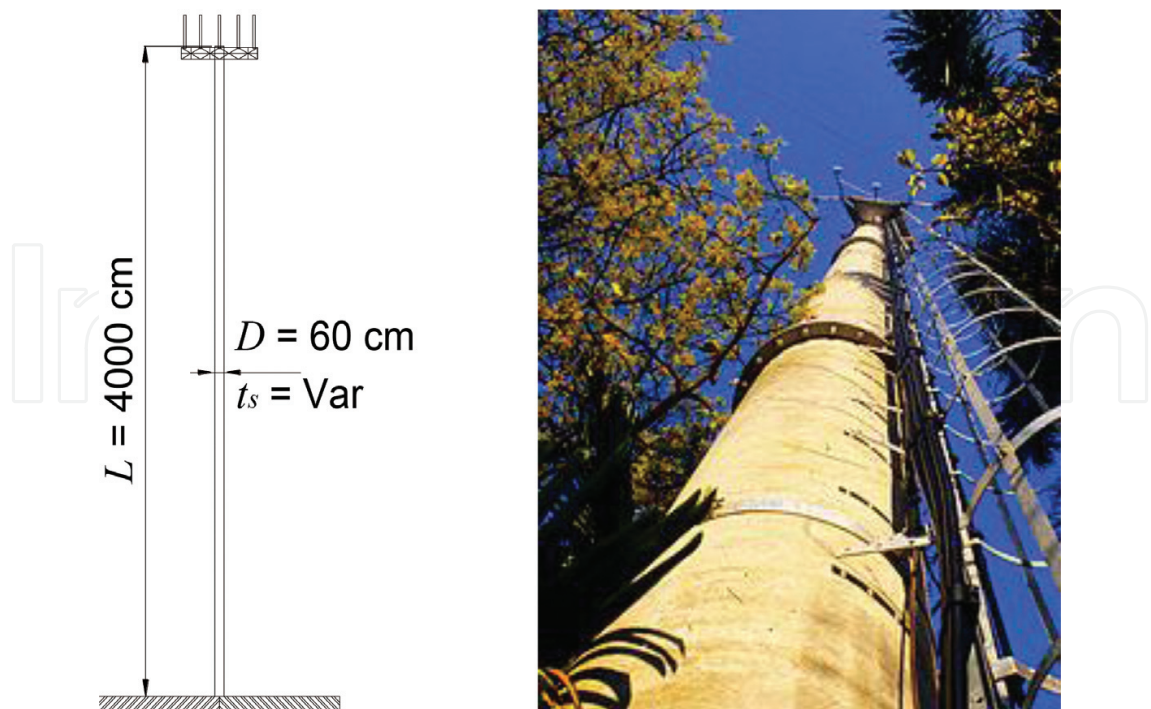


Figure 9. A column as a mast transition system.

The structure also has an array of antennas and accessories, such as a platform, stairs, cables, and mats (characteristics shown in **Table 1**), which exert compressive forces. It is important to mention that the viscous parameter was adjusted so that the deformations converged at 90 days (**Figure 10(a)**), as observed by [8]. With this, it was possible to obtain the variable modulus of elasticity  $E(t)$  (**Figure 10(b)**). The gravitational ( $g$ ) acceleration was assumed to be  $9.806650\text{ m/s}^2$ .

Since this is a cylindrical concrete reinforcement structure, it is necessary to take into account the presence of reinforcement bars at the moment of inertia of the cross-sectional area, which must be done by homogenizing the concrete area. Considering a circular ring cross section with external diameter  $D$ ; thickness of the wall  $t_s$ ;  $s$  relative to the considerate segment of the structure; a reinforcement bar  $b_i$  any occupies a position  $i$  in the section defined by  $R_{bi}$  and  $\theta_i$ ,

Dispositive	Height	Weight
Pole	from 0 to 40 m	25.48 kN/m <sup>3</sup>
Stair	from 0 to 40 m	0.15 kN/m
Cables	from 0 to 40 m	0.25 kN/m
Platform and supports	40 m	4.90 kN
Antennas	40 m	1.88 kN

Table 1. Structure’s characteristics and devices.

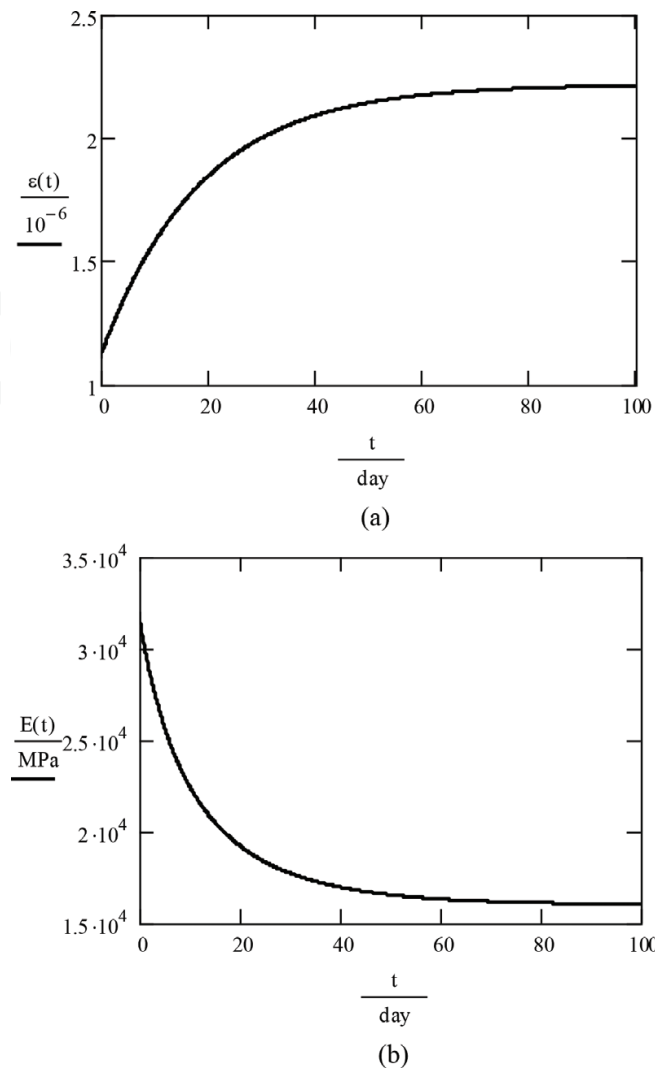


**Figure 10.** Deformation and modulus of elasticity over time. (a) Deformation, (b) Elasticity.

as shown in **Figure 11**.  $R_{bi}$  determines the center position of each bar in relation to the section center.  $c'$  is the concrete cover of the reinforcement and  $d_{bi}$  is the diameter of the  $i$  bar.

$$R_{bi} = \frac{D}{2} - c' - \frac{d_{bi}}{2}. \quad (21)$$

As  $\theta_i$  is the independent variable, the distance between the center of each bar relative to the axis center of inertia of the section is

$$y(\theta_i) = \sin(\theta_i)R_{bi}. \quad (22)$$

The spacing between the center of each bar section was obtained for  $sp. = 2\pi R_{bi}/n_{bi}$ , where  $n_{bi}$  is the number of bars of the reinforcement steel. The angular phase shift between them is  $\Delta\theta = sp/R_{bi}$ .

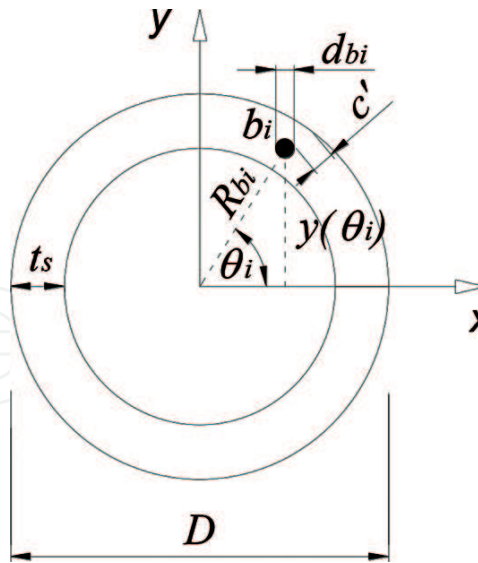


Figure 11. Parameters for homogenizing concrete section.

Since the  $\theta_i$  varies from 0 to  $2\pi$  at intervals defined by  $\Delta\theta$ , the total inertia of the steel bars in relation to the section of the structure could be obtained by the theorem of parallel axes with the expression (14).

$$I_s = \sum_{\theta} \left( \frac{\pi d_{bi}^4}{64} + y(\theta_i)^2 \frac{\pi d_{bi}^2}{4} \right). \quad (23)$$

The homogenized moment of inertia of the steel bars will thus be:

$$I_{shom} = \sum_{\theta} I(\theta_i) \left( \frac{E_s}{E_c} - 1 \right). \quad (24)$$

The total homogenized inertia of the section will be obtained by  $I_{tot} = I + I_{shom}$ , with  $I$  being the inertia of the circular section,  $I = \pi/64 [D^4 - (D - 2t_s)^4]$ . Thus, to find a factor  $F_s$ , which multiplies the nominal inertia of the section in terms of total steel inertia, the homogenized section is made by  $F_s = 1 + (I_{shom}/I_{tot})$ . Factors of homogenizing, the structural properties and the geometry of the structure are shown in **Table 2**.

Considering that the actual structure has variable proprieties along the height, the expressions (16), (17) and (18) must be resolved for each interval defined by structural geometry. The frequency was calculated for the 90th day according to Eq. (10) (see **Figure 12**).

**Figure 13(a)** shows the structural frequency over time, for a height limit of losing stability, calculated for the 90th day, considering viscoelasticity ( $L = 50.6975$  m). To a height of 57.0000 m, for example, the behavior of **Figure 13(b)** is found, with the structural collapse occurring on the 60th day. The height limit without viscoelasticity (instant 0) is 71.29 m, a frequency of 0.0000 Hz.

Similar simulations for evaluation of the viscoelasticity can be found in [20, 21].

Height $L_s$ (m)	External diameter $D$ (cm)	Thickness $t_s$ (cm)	Number of bar ( $n_{bi}$ )	Bar diameter $d_{bi}$ (mm)	Factors of homogenizing $F_s$
40	60	10	20	13	1.0963
39	60	10	20	13	
38	60	10	20	13	
37	60	10	20	13	
36	60	10	20	13	
35	60	10	20	13	
34	60	10	20	13	
33	60	10	20	13	
32	60	10	20	13	
31	60	13	20	13	1.0869
30	60	12	15	16	1.0995
29	60	11	15	16	1.1029
28	60	11	15	16	
27	60	11	15	16	
26	60	11	15	16	
25	60	11	16	16	1.1091
24	60	11	17	16	1.1153
23	60	11	18	16	1.1214
22	60	11	19	16	1.1274
21	60	11	20	16	1.1334
20	60	14	20	16	1.1230
19	60	15	15	20	1.1374
18	60	16	15	20	1.1354
17	60	13	16	20	1.1512
16	60	13	16	20	
15	60	13	17	20	1.1594
14	60	13	18	20	1.1675
13	60	13	19	20	1.1755
12	60	13	19	20	
11	60	13	20	20	1.1833
10	60	13	22	20	1.1987
9	60	16	22	20	1.1889
8	60	16	15	25	1.1961
7	60	17	15	25	1.194
6	60	14	16	25	1.2132
5	60	14	16	25	
4	60	14	17	25	1.2241
3	60	14	17	25	
2	60	14	17	25	
1	60	18	17	25	1.2136
0	60	18	17	25	

**Table 2.** Structural properties and homogenizing factors of sections.

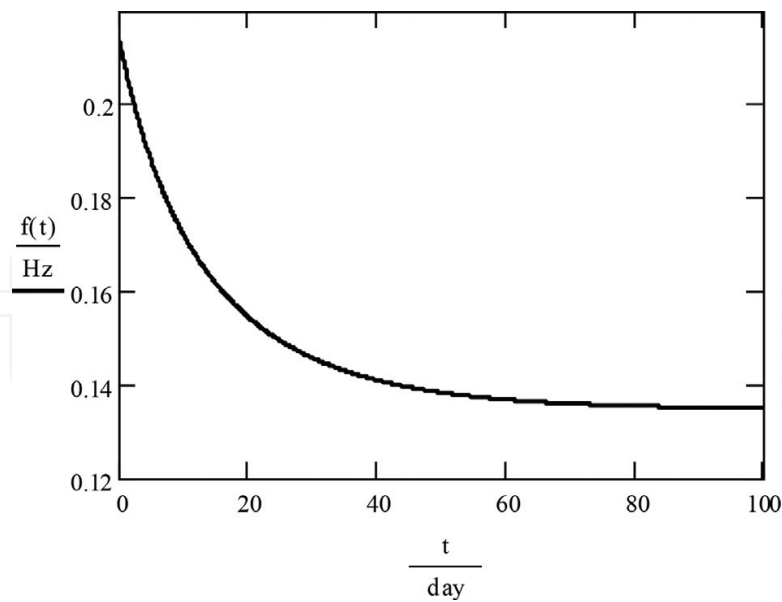


Figure 12. Frequency variation on structure at 90 days.

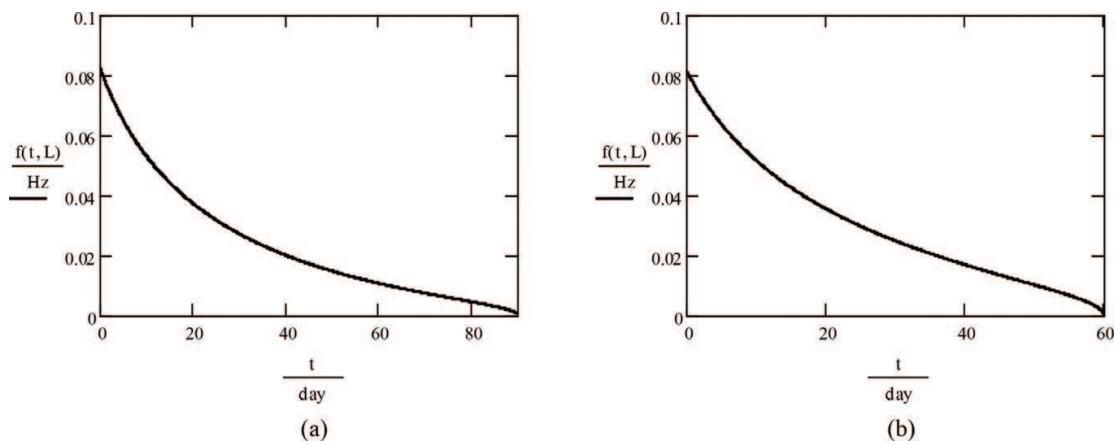


Figure 13. Structural frequency on height of losing stability. (a)  $L = 50.6975\text{ m}$ —Collapse on the 90th day, (b)  $L = 57.0000\text{ m}$ —Collapse on the 60th day.

## 5. Conclusions

### Simulation 1

- In this work, a numerical simulation of a reinforced-prestressed concrete beam as a support for rotating machines was performed.
- For the vibration analysis, the viscoelasticity, which is an intrinsic material property, was introduced due to the slenderness of the beam, revealing a resonant regime not foreseen in the linear analysis (without viscoelasticity).

- The effect of geometric stiffness produced by the horizontal loading and the corresponding possibility of introducing resonant regimes in the structural support system were demonstrated by calculating their frequencies.
- It can be concluded, therefore, that due to the increase of the axial compressive force, resonance conditions can occur, as represented by the intersection of the curves in **Figure 7**. In the present study, resonance occurs when the axial compression force reaches 210 kN at 10 days. Other instants might also be considered.
- Since the force of post-tension decreases the stiffness of the beam, this can lead to the resonant regime if it has not been previously evaluated in the structural analysis.
- The technique studied in this chapter offers an efficient tool to provide the removal of the support structure of that unwanted regime, avoiding the production of harmful effects on the equipment, fabricated products, and work environment of the operators.
- In further work, it is necessary to introduce normative criteria, perform experimental activity, and evaluate the influence of the prestressing bar stiffness on the structural response.

#### Simulation 2

- The modulus of elasticity calculated by Eq. (6) on the ninth day was 16027.64 MPa, which represents a decrease of 49.81% in relation to the initial value of 31931.05 MPa.
- The frequency of the structure calculated at the initial moment was 0.215715 Hz, and on the 90th day, of 0.135021 Hz, representing a reduction of 37.41%.
- The simulated structure finds its limit of stability when reaching 50.6975 m, collapsing at 90 days. If the viscoelastic effect were not considered, the height limit would be 71.29 m, 20.47% above the first one. The obtained result was taken for an exactitude of five decimal significant algorithms ( $f = 0.00000$ ).
- The previous aspect is relevant because if the height were considered between the limit established without the viscoelasticity and that defined with it, the structure would collapse before the end of 90 days in service. For a height of 57 m, for example, the collapse would occur 60 days after being loaded.
- Others rheological models for representing viscoelastic behavior can be tested in order to evaluate the frequency of a column of reinforced concrete as well as criteria from regulatory codes.
- The critical load of buckling can be obtained by using the same process present in this work and comparing it to other tools for calculations as, for example, finite element method (FEM).

#### Acknowledgements

This work was supported by the National Council for Scientific and Technological Development (CNPq) from Brazil by process 443,044/2014–7 in Call MCTI/CNPQ/Universal 14/2014.



## Author details

Alexandre de M. Wahrhaftig<sup>1\*</sup>, Reyolando M. L. R. F. Brasil<sup>2</sup> and  
Lázaro S. M. S. C. Nascimento<sup>1</sup>

\*Address all correspondence to: alixa@ufba.br

1 Department of Construction and Structures Rua Aristides Novis, Polytechnic School,  
Federal University of Bahia (UFBA), Salvador, BA, Brazil

2 Department of Structural and Geotechnical Engineering, University of São Paulo (USP)  
Polytechnic School, Cidade Universitária, São Paulo, SP, Brazil

## References

- [1] Wahrhaftig AM, Brasil RMLRF, Balthazar JM. The first frequency of cantilever bars with geometric effect: a mathematical and experimental evaluation. *Journal of the Brazilian Society of Mechanical Sciences and Engineering*. 2013;**35**:457-467. DOI:10.1007/s40430-013-0043-9
- [2] Wahrhaftig AM, Brasil RMLRF. Representative experimental and computational analysis of the initial resonant frequency of largely deformed cantilevered beams. *International Journal of Solids and Structures*. 2016;**102-103**:44-55. DOI: 10.1016/j.ijsolstr.2016.10.018
- [3] Wahrhaftig AM, Brasil RMLRF. Vibration analysis of mobile phone mast system by Rayleigh method. *Applied Mathematical Modelling*. 2016;**42**:330-345. DOI: 10.1016/j.apm.2016.10.020
- [4] Wahrhaftig AM, Brasil RMLRF. Initial undamped resonant frequency of slender structures considering nonlinear geometric effects: The case of a 60.8 m-high mobile phone mast. *Journal of the Brazilian Society of Mechanical Sciences and Engineering*. 2016;**39**(3): 725-735. DOI: 10.1007/s40430-016-0547-1
- [5] Clough RW, Penzien J. *Dynamic of Structures*. 2nd ed. Taiwan: McGraw Hill International Editions; 1993
- [6] Findley WN, Lai JS, Onaran K. *Creep and Relaxation of Nonlinear Viscoelastic Materials, With an Introduction to Linear Viscoelasticity*. New York: Dover Publications, Inc.; 1989
- [7] Leohard F, Mong E. *Constructions of Concrete – Basic Principles for Dimensioning of Concrete Structures*. 1st. ed. Vol. 1, Rio de Janeiro: Livraria Interciência; 1977
- [8] Mehta PK, Monteiro PJM. *Concrete: Structure, Properties and Materials*. São Paulo: PINI; 1994

- [9] Armijo NC, Paola MD, Pinnola FP. Fractional characteristic times and dissipated energy in fractional linear viscoelasticity. *Communications in Nonlinear Science and Numerical Simulation*. 2016;**37**:14-30. DOI:10.1016/j.cnsns.2016.01.003
- [10] Wahrhaftig AM, César SF, Brasil RMLRF. Creep in the fundamental frequency and stability of a slender wooden column of composite section. *Revista Árvore*. 2016;**40**(6):1129-1140. DOI:10.1590/0100-67622016000600018
- [11] Oliveira AW. Uso do concreto protendido em pontes: Estudo de Caso da Nova Ponte Sobre o Rio São Francisco na BR-101. V Encontro Nacional de Estudantes de Engenharia Civil, Porto Seguro; 2016. (In Portuguese)
- [12] Calduro EL. Em favor da leveza. *Revista Técnica, PINI*, n. 26; 1997. (In Portuguese)
- [13] Jost DT. Análise de peças fletidas com protensão não aderente pelo método dos elementos finitos. 152 p. Dissertação (Mestrado em Engenharia Civil) – Universidade Federal do Rio Grande do Sul. Porto Alegre, 2006. (In Portuguese)
- [14] Rayleigh. *Theory of Sound* (two volumes). New York: Dover Publications, re-issued;1877
- [15] Temple G, Bickley WG. *Rayleigh's Principle and its Applications to Engineering*. London: Oxford University Press, Humphrey Milford;1933
- [16] Leissa AW. The historical bases of the Rayleigh and Ritz methods. *Journal of Sound and Vibration*. Nov. 2005;**287**(4–5):961-978
- [17] Levy R, Spillers WR. *Analysis of Geometrically Nonlinear Structures*. New York: Chapman & Hall; 1995
- [18] National Regulatory Standard (Norma Brasileira), NBR – 6118–Design of Structural Concrete–Procedure. Rio de Janeiro: Brazilian National Standards Association (Associação Brasileira de Normas Técnicas, ABNT); 2014
- [19] Wahrhaftig AM. Analysis of the first modal shape: Using two case studies. *International Journal of Computational Methods*. 2018;**15**(3):1840019 (14 pages). DOI: 10.1142/S0219876218400194
- [20] Wahrhaftig AM, Brasil RMLRF. Essay on Creep in Vibration Columns (Ensaio sobre a fluência na vibração de colunas), Paper ID 002, Congress on Numerical Methods in Engineering CMN2015, Lisboa; 2015
- [21] Wahrhaftig AM. Rayleigh with Viscoelasticity Applied to a Highly Slender 40-m-high Concrete Mast, Congress on Numerical Methods in Engineering CMN2017, July 3–5, Valencial; 2017

